Tellus **000**, 000–000 (0000) Printed 15 November 2008 (Tellus LaTeX style file v2.2)

Probabilistic hindcasts and projections of the coupled climate, carbon cycle, and Atlantic meridional overturning circulation system: A Bayesian fusion of century-scale observations with a simple model

By NATHAN M. URBAN[1]* and KLAUS KELLER[1],

[1] *Department of Geosciences, Penn State, University Park, PA 16802*

15 November 2008

For Peer Review

ABSTRACT

How has the Atlantic Meridional Overturning Circulation (AMOC) varied over the past centuries and what is the risk of an anthropogenic AMOC collapse? Current AMOC projections have broken important new ground, but either use only a small subset of the relevant observational constraints or sample mostly in the region around the best parameter estimates.

Here we improve on previous studies by (i) greatly expanding the considered observations and (ii) carefully sampling the tail areas of the parameter probability distribution (pdf). We use a Bayesian inversion to fuse observations covering the last two centuries with a simple model of the coupled climate, carbon cycle, and AMOC systems to derive multi-century hindcasts and projections.

Our hindcasts show considerable skill in representing the observational constraints. We show that robust AMOC risk estimates can require carefully sampling the tails of the pdfs. The probability of experiencing an AMOC collapse within the 21st century is less than ten percent in our model for a business-as-usual emissions scenario. However, the probability of crossing a forcing threshold during the 21st century and committing to a future collapse is 40 percent in this scenario. The probability of an AMOC collapse within the next two centuries exceeds 50 percent.

* Corresponding author.

e-mail: nurban@psu.edu

© 0000 Tellus

1 Introduction

Fossil fuel consumption has driven atmospheric carbon dioxide (CO_2) concentrations far beyond the range experienced by previous civilizations. This anthropogenic perturbation of the Earth system has already committed future generations to considerable climate change, with potentially profound and irreversible effects on ecosystems and human society (Adger et al., 2007; Alley et al., 2007). Here we focus on a key example of such an anthropogenic climate change impacts: a potential collapse of the Atlantic meridional overturning circulation (AMOC) (Stouffer et al., 2006). An AMOC collapse would likely have nontrivial economic impacts, for example by changes in global temperature and precipitation patterns (Keller et al., 2000; 2004; Link and Tol, 2004; Vellinga and Wood, 2002).

The AMOC is sensitive to anthropogenic climate forcings (Meehl et al., 2007). Current surface temperature patterns are strongly influenced by the Gulf stream and the North Atlantic current (Vellinga and Wood, 2002). These surface currents transport heat from the tropics to higher northern latitudes in the Atlantic basin. The heat loss from the surface waters to the atmosphere cools the waters and acts to increase the water density. In addition, the formation of sea ice at high latitudes acts to increase the salinity of the surface waters due to brine rejection. The decrease in temperature and the increase in salinity both increase the water densities. Surface waters that are denser than the underlying water masses sink. This deepwater formation process is an important part of a global deepwater circulation system that is often referred to as the "global conveyor belt" (Broecker, 1991).

The conveyor belt circulation may collapse in response to anthropogenic climate forcings (Meehl et al., 2007; Stommel, 1961). Anthropogenic greenhouse gas emissions are projected to increase surface temperatures and net freshwater input in the North Atlantic (Meehl et al., 2007). Both of these factors drive a decrease of the surface water densities. A decrease in the surface water density acts to decrease the density gradient between surface and deepwaters and hence acts to decrease the AMOC intensity.

The AMOC may exhibit a threshold response to anthropogenic forcing due to positive feedbacks (Stocker et al., 2001; Stommel, 1961). One key positive feedback destabilizing the AMOC is driven by the net freshwater input in the North Atlantic region (Baumgartner and Reichel, 1975; Stommel, 1961). Consider, for example, an AMOC weakening due to the anthropogenic climate forcing as discussed above. This AMOC weakening results in a slowdown of the surface currents transporting waters to the deepwater formation sites, which

For Peer Review

increases the transit time of these surface waters through the region of net freshwater inputs from the atmosphere. The increased transit time decreases the salinity of the surface waters. The decrease in salinity decreases the water density, which further weakens the AMOC through a positive feedback loop.

Oceanic observations show some tantalizing evidence for an AMOC slowdown over the last few decades. For example, repeated transects at 26 °N (Bryden et al., 2005) have been interpreted as a 30 percent AMOC slowdown over the last four decades. In addition, salinities in the northern North Atlantic Ocean have decreased considerably since the mid-1960s (Curry and Mauritzen, 2005). The evidence for a potential AMOC weakening is, however, not straightforward to interpret. For example, recent measurements at high temporal resolution suggest that the AMOC decrease reported by Bryden et al. (2005) may be due to unforced internal variability, as opposed to being a response to anthropogenic forcing (Cunningham et al., 2007). These observations suggest the distinct possibility of a considerable AMOC sensitivity to radiative forcing.

Current projections of the AMOC are deeply uncertain (Keller, Schlesinger and Yohe, 2007; Keller and McInerney, 2008; Meehl et al., 2007). There is disagreement in the literature regarding the probability of such an outcome. The Intergovernmental Panel on Climate Change (IPCC) has recently stated that "it is very unlikely that the MOC will undergo a large abrupt transition during the 21st century", implying a probability of less than ten percent (Alley et al., 2007). Previous studies deriving probabilistic AMOC projections have broken important new ground but are still silent on key questions. The first, and arguably simplest, class of AMOC projections uses very simplified models (e.g., box or 2.5-dimensional models) with rather limited use of observational constraints (Knutti et al., 2003; Yohe et al., 2006). The use of low-dimensional AMOC models enables the extensive sampling of the large parameter space and to explore the tails of the associated probability density function (pdf). The disadvantage of using these simple models is that the resulting scenarios hinge critically on the assumption that the neglected feedbacks, for example through changes in the respiration of the soil carbon pool (Friedlingstein et al., 2006), are unimportant. The second class of AMOC projections is based on EMICs with considerably improved representation of relevant processes and feedbacks (e.g., Challenor et al., 2006). However, studies using EMICS sample the tails of the parameter probability density function rather sparsely (Challenor et al., 2006). The third class of AMOC projections is based on high resolution coupled Atmosphere Ocean General Circulation Models (AOGCM) (e.g., Schneider et al., 2007;

For Peer Review

Meehl et al., 2007). This approach has the advantage of being based on more realistic models, but the large computational costs of AOGCMs precludes at this time to exhaustively sample the tails of the parameter distributions. In summary, robust probabilistic AMOC hindcasts and projections require at least two key properties: (i) they have to be based on mechanistically sound models that include key feedbacks, and (ii) they need to represent the full parametric uncertainty (including the tails of the joint probability density function) given relevant observational constraints.

Ideally, one would fuse all of the available and relevant constraints into all available high resolution AOGCMs in a Bayesian model averaging sense (Draper, 1995; Hoeting et al., 1999). However, this is not possible at this time due to prohibitive computational requirements. Here we take a less ambitious approach and fuse a subset of relevant observations with a simple model of the coupled carbon, climate, and AMOC system. The results from this proof-of-concept study are hence subject to several caveats (discussed below). The main advances of our study compared to previous research are the expansion of the considered observational constraints, the expanded sampling of the tails of the parameter probability density function, and the correction for the effects of autocorrelated residuals.

For Peer Review

2 Model

Past and future AMOC strengths depend on an intricate interplay of radiative climate forcings (e.g., due to solar variability, volcanic and industrial aerosols, or greenhouse gases such as carbon dioxide), the resulting changes in surface air temperatures and precipitation patters, and the resulting AMOC changes. Deriving probabilistic AMOC hindcasts and projections therefore requires to couple models of (i) the carbon cycle, (ii) surface air temperature and precipitation patterns, and (iii) the AMOC response. These model components and their coupling are described below.

2.1 Climate module

We use an energy balance model of the atmosphere coupled to a one-dimensional diffusive ocean model to calculate global temperature and ocean heat content. Specifically, we use the ACC2/DOECLIM model (Kriegler, 2005; Tanaka and Kriegler, 2007). In this model, the

land and sea temperatures T_L and T_S are determined by energy balance conditions,

$$\dot{T}_L = (a_{\Gamma,L} C_A + C_L)^{-1} \times \left[Q_L - \lambda_L T_L - \frac{k}{f_L} \left(T_L - b_{SI} \frac{a_{\Gamma,S}}{a_{\Gamma,L}} T_S \right) \right], \quad (1)$$

$$\dot{T}_S = (a_{\Gamma,S}\, b_{SI} C_A + c_V z_S)^{-1} \times \left[Q_S - \lambda_S - \frac{k}{1-f_L} \left(b_{SI} \frac{a_{\Gamma,S}}{a_{\Gamma,L}} T_S - T_L \right) - F_O \right]. \quad (2)$$

Here the overdot denotes the time derivative, C and c are land/air and water heat capacities, Q are radiative forcings (at the top of the atmosphere), λ are climate feedback parameters, a_Γ are surface-troposphere couplings, b_{SI} is a surface-mixed layer coupling, k is a land-sea heat exchange coefficient, F_O is the heat flux into the interior ocean, z_S is the depth of the ocean mixed layer, and f_L is the land fraction of the Earth's surface area.

The uptake of heat into the interior ocean is governed by a one-dimensional diffusion equation,

$$\dot{T}_O(z,t) = \kappa_V \frac{\partial^2}{\partial z^2} T_O(z,t), \quad (3)$$

subject to the boundary conditions that $T_O = T_S$ at the surface ($z = 0$) and the heat flux into the ocean floor ($z = z_B$) vanishes, where T_O is the ocean temperature as a function of depth and time and κ_V is the vertical diffusivity of heat. This diffusion equation has an exact analytic solution which is approximated in DOECLIM by a series expansion.

The CO_2 radiative forcing of the climate is given by the logarithmic response to increases in atmospheric CO_2 as predicted by the carbon module. The other radiative forcings (e.g., non-CO_2 greenhouse gases, solar irradiance, volcanism, and tropospheric aerosols) are taken from Kriegler (2005). We account for the considerable uncertainty in the magnitude of the aerosol forcing feedback (Hegerl et al., 2006) by applying a multiplicative scale factor α, which is estimated from the observations.

2.2 AMOC box model

We approximate the AMOC by a simple box model developed by Zickfeld et al. (2004), forced with temperature change from the climate module. The Atlantic Ocean is represented by four well-mixed boxes: the southern, tropical, and northern surface waters, and the deep water. The boxes are connected sequentially so that surface currents flow from south to north by way of the tropics, overturn, and return to the south as deep water. This self contained cycle ignores the transport of water outside of the Atlantic.

For Peer Review

The dynamics of the box temperatures T_i and salinities S_i are governed by a simple system of coupled first order ordinary differential equations:

$$\dot{T}_S = \frac{m}{V_S}(T_D - T_S) + \lambda_S(T_S^* - T_S)\,, \tag{4}$$

$$\dot{T}_N = \frac{m}{V_N}(T_T - T_N) + \lambda_N(T_N^* - T_N)\,, \tag{5}$$

$$\dot{T}_T = \frac{m}{V_T}(T_S - T_T) + \lambda_T(T_T^* - T_T)\,, \tag{6}$$

$$\dot{T}_D = \frac{m}{V_D}(T_N - T_D)\,, \tag{7}$$

$$\dot{S}_S = \frac{m}{V_S}(S_D - S_S) + \frac{S_0 F_{ST}}{V_S}\,, \tag{8}$$

$$\dot{S}_N = \frac{m}{V_N}(S_T - S_N) - \frac{S_0(F_N + F_{TN})}{V_N}\,, \tag{9}$$

$$\dot{S}_T = \frac{m}{V_T}(S_S - S_T) - \frac{S_0(F_{ST} - F_{TN} - F_T)}{V_T}\,, \tag{10}$$

$$\dot{S}_D = \frac{m}{V_D}(S_N - S_D)\,, \tag{11}$$

where T_i^* are the temperatures to which the boxes relax, λ_i are thermal coupling constants, V_i are box volumes, and F_i are external freshwater fluxes into surface boxes. (Here the southern box temperature T_S is not to be confused with the sea temperature T_S in the DOECLIM climate model, Eq. 2.) F_N represents the meltwater flux into the North Atlantic, and F_T represents the flux out of the tropical Pacific into the North Atlantic (Latif et al., 2000). F_{ij} are freshwater fluxes between surface boxes, and S_0 is a reference salinity. The key observable parameter in this analysis is the meridional volume transport rate (overturning) between the southern and northern boxes, referred to henceforth as the AMOC strength, given by

$$m = k[\beta(S_N - S_S) - \alpha(T_N - T_S)]\,, \tag{12}$$

where k is a hydraulic constant and α and β are thermal and haline expansion coefficients. If the model produces an AMOC reversal, m is set to zero, representing an AMOC collapse.

The relaxation temperatures and freshwater fluxes of the surface boxes are time dependent functions of the global temperature forcing ΔT, which is calculated by the climate module:

$$T_S^* = T_{S_0}^* + p_S \Delta T\,, \tag{13}$$

$$T_N^* = T_{N_0}^* + p_N \Delta T\,, \tag{14}$$

$$T_T^* = T_{T_0}^* + p_T \Delta T\,, \tag{15}$$

For Peer Review

and

$$F_N = h_N p_{NH} \Delta T \,, \tag{16}$$

$$F_T = -h_T p_T \Delta T \,, \tag{17}$$

$$F_{ST} = F_{ST_0} + h_{ST} p_{SH} \Delta T \,, \tag{18}$$

$$F_{TN} = F_{TN_0} + h_{TN} p_{NH} \Delta T \,, \tag{19}$$

where the $T^*_{i_0}$ are unforced relaxation temperatures, the p_i are linear pattern scaling coefficients to estimate regional Atlantic and hemispheric temperatures from global temperatures, and the h_i give hydrological sensitivity to warming.

One key uncertain parameter affecting the AMOC response to anthropogenic climate forcing is the North Atlantic hydrological sensitivity, $h \equiv h_N$, which gives the change in freshwater flux into the northern box for a given change in surface air temperature. A high sensitivity implies a greater AMOC sensitivity to anthropogenic forcing (Zickfeld et al., 2004).

For hindcasts and calibration we use the deterministic box model described above. For future projections we follow Knutti and Stocker (2002) to represent unresolved stochastic variability (e.g., weather) by randomly perturbing each year the annual temperatures of the three surface boxes. The magnitude of the temperature perturbation, which is the same for all three boxes, is determined by fitting the unforced AMOC strength so that its stochastic time series properties (variance and lag-1 autocorrelation coefficient) approximate that of an unforced run of the GFDL AOGCM (Manabe and Stouffer, 1994).

2.3 Carbon cycle model

We couple a carbon cycle model to the climate module. Temperature changes affect terrestrial and ocean carbon sources and sinks. In turn, these sources and sinks alter the atmospheric carbon dioxide concentration which forces the climate. To model the carbon cycle we use a nonlinear impulse response approximation to the Hamburg AOGCM (Hooss et al., 2001), as modified by Ricciuto et al. (2008). The model structure and the calibration using oceanic, atmospheric, and ice core observations are detailed in Ricciuto et al. (2008). We hence give here just a brief overview.

The carbon cycle module considers the terrestrial as well as oceanic carbon cycles. There are four terrestrial carbon pools: leafy vegetation, living wood, detritus, and humus (soil carbon). The ocean model of carbon uptake has four layers: a mixed atmosphere/surface

For Peer Review

layer and three deeper layers. The three key parameters we alter in the carbon cycle model are the carbon fertilization parameter β, the respiration sensitivity Q_{10}, and the thermocline transfer rate η. The carbon fertilization parameter affects the magnitude of the atmospheric CO_2 flux taken up by living plants (net primary productivity) due to the influence of CO_2 concentrations on plant growth. The respiration sensitivity affects the increase in atmospheric CO_2 due to temperature accelerated organic decay. The thermocline transfer rate governs the rate at which dissolved carbon diffuses from the surface into the deep ocean.

3 Data

3.1 Forcings

We consider CO_2 emissions from (i) fossil fuel burning, (ii) cement production (both taken from Marland et al. (2004), and (iii) land-use changes (from Jain and Yang, 2005, based on the land-use estimate of Ramankutty and Foley, 1999). Because the DOECLIM forcings have not been updated past the year 2000, projected forcings are used after 2000, including in the hindcast calibration period. Future forcings from business-as-usual (BAU) CO_2 emissions, from non-CO_2 greenhouse gas, and anthropogenic aerosols are adopted from Nordhaus (2007). Forcings due to volcanic aerosols are projected using a simple stochastic time series model. Specifically, we assume that the time series is stationary and bootstrap resample the historic forcing. Stochastic projection is disabled during the model calibration. The solar forcing is projected by imposing a fitted sine curve model with the observed 11-year solar cycle on the average forcing to solar cycles 22 and 23. The temperature projections are derived from the climate module with autocorrelated process noise superimposed to simulate interannual variability. The AMOC model is forced with the hindcast and projected temperatures.

3.2 Observational constraints

We use six different observational data sets to calibrate the model: atmospheric CO_2 concentrations from Mauna Loa (Keeling and Whorf, 2005), (ii) CO_2 concentrations from the Law Dome ice core (Etheridge et al., 1996), (iii) estimates of the anthropogenic carbon fluxes into the oceans based on chlorofluorocarbon measurements (McNeil et al., 2003), (iv) a synthesis data set of combined land and marine global temperatures (Brohan et al., 2006), (v) estimates of oceanic heat uptake (Gouretski and Koltermann, 2007), and (vi)

For Peer Review

AMOC strength estimates by Bryden et al. (2005) and Cunningham et al. (2007), with error estimates derived from Kanzow et al. (2007) and Lumpkin and Speer (2007).

4 Inversion method

We use a Bayesian inversion technique based on a Markov Chain Monte Carlo (MCMC) algorithm (Metropolis et al., 1953; Hastings, 1970) to fuse these observational constraints with the model. The method accounts for potential autocorrelation in the residuals using a modified likelihood function (Zellner and Tiao, 1964). Specifically, the CO_2 time series from Mauna Loa and the Law Dome as well as the global mean surface temperature anomalies and the oceanic heat uptake are taken to be of unknown variance and autocorrelation. We assume these distributional parameters to be independent of each other and of the model parameters. We also estimate the initial values in the temperature, ocean heat, and AMOC time series. The estimated parameters with their prior distributions are detailed in Table 1. For the AMOC time series, we adopt the published variance estimates (Bryden et al., 2005; Kanzow et al., 2007; Lumpkin and Speer, 2007) and neglect potential autocorrelation. Due to their sparsity, the ocean carbon flux data points are assumed to be independent (and identically distributed) with normal observational errors adopted from McNeil et al. (2003). The hindcast calibration period used in the inversion is the years 1850–2007.

The calibrated parameters found in the inversion are used to probabilistically project future climate observables. The hindcasts and projections have observational/process noise superimposed. The temperature, ocean heat, and CO_2 errors and autocorrelations are estimated as above, with the CO_2 error assumed the same as the instrumental time series. The AMOC error is assumed to be ± 6 Sv (1σ) in hindcasts (1850–2007) following Bryden et al. (2005), and 2 Sv in projections (after 2007) following Cunningham et al. (2007).

5 Results and discussion

The hindcasts of mean surface air temperatures, oceanic heat anomalies, atmospheric CO_2 concentrations, and AMOC strength show considerable skill. For example, the observed air temperature cooling after the Agung and Pinatubo volcanic eruptions (in 1963 and 1991, respectively) are reasonably well reproduced in the hindcasts (Figure 1). There is a slight suggestion that a similar pattern is seen in the oceanic heat anomaly, but this signal is relatively small compared to the data uncertainties and the magnitude of the

For Peer Review

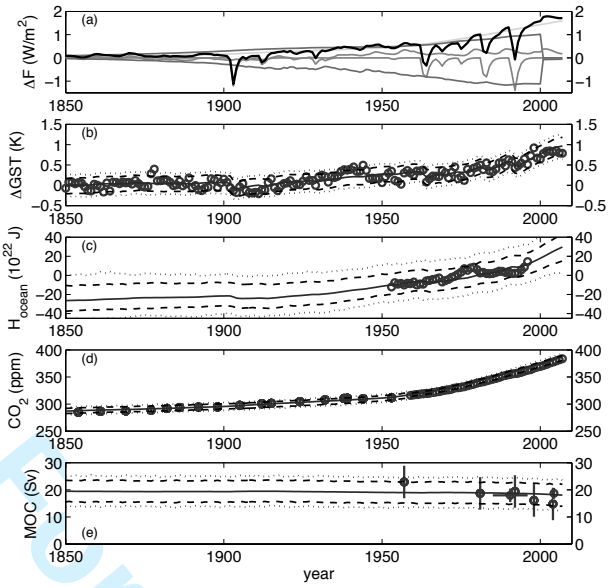

Figure 1. Historic forcings and probabilistic hindcasts of global mean surface temperature anomalies, oceanic heat anomaly, atmospheric CO_2 concentrations, and AMOC strength. The thick black line in the top panel is the total radiative forcing. The thin gray lines are, from top to bottom, CO_2, non-CO_2 greenhouse gases, solar variability, volcanic aerosols, and anthropogenic aerosols. The forcing data are adopted from Kriegler (2005). CO_2 and aerosol forcings are taken from the best fit hindcast. In the remainder of the panels, the observational constraints are shown by open circles. The best fit (maximum posterior probability) model outputs are shown by solid curves, and the dashed and dotted curves are 90% and 98% predictive credible intervals. The vertical error bars in panel E represent one standard deviation of the reported observation errors (Bryden et al., 2005; Kanzow et al., 2007; Lumpkin and Speer, 2007).

data-model residuals. The anthropogenic trend in atmospheric CO_2 concentrations is large compared to the observation uncertainties, resulting in a high signal-to-noise ratio. The relatively large signal-to-noise ratio in the CO_2 hindcasts allows relatively well-constrained parameter estimates (discussed below) and thereby relatively tightly constrained projections. The signal-to-noise ratio decreases from the CO_2 observations to the observations of surface air temperature, oceanic heat anomaly, and the AMOC intensity.

Parameter estimates associated with the high signal-to-noise ratio are considerably sharpened compared to their prior estimates (Figure 2). This is the case, for example, for the CO_2 fertilization factor and the climate sensitivity. In contrast, the estimates for the hydrological sensitivity is much less constrained by the observations. The shape of the climate sensitivity estimate with the elongated right tail (i.e., the positive skewness) is similar to recent estimates (Meehl et al., 2007). The considered AMOC observations have very little power to sharpen the prior estimate of the hydrological sensitivity, consistent with the findings of Keller and McInerney (2008).

Some of the parameter estimates show strong correlations (Figure 3). For example, estimates of the ocean thermocline exchange rate for CO_2 and the CO_2 fertilization factor are negatively correlated (Figure 3, row 2, column 2). This finding is similar to the findings

For Peer Review

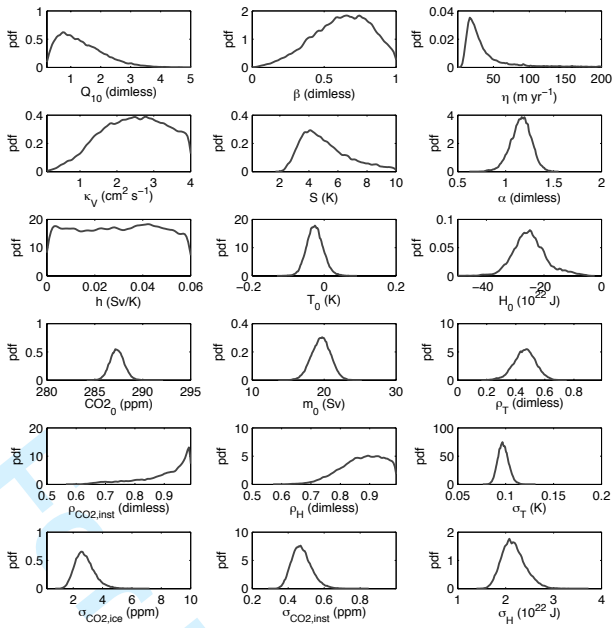

Figure 2. Marginal probability density functions of the estimated parameters. The axis range represents the lower and upper bounds of the prior probability density function.

of Ricciuto et al. (2008) and is expected because an increased thermocline exchange rate requires a decreased CO_2 fertilization factor to result in the same atmospheric CO_2 observations. A second example is the positive correlation between the climate sensitivity and the aerosol scaling factor (Figure 3, row 5, column 5). This positive correlation is expected because a higher climate sensitivity can be masked by a stronger (negative) climate forcing by aerosols (Forest et al., 2002). A third example is the correlation between the climate sensitivity and the vertical diffusivity of heat in the ocean (Figure 3, row 4, column 4). This correlation is expected to be positive when observing surface temperatures, and negative when observing ocean heat content (Urban and Keller, 2008). The correlation is net positive in our study, suggesting that surface temperature provides a relatively stronger constraint on climate sensitivity than ocean heat, consistent with the signal-to-noise ratios present in those data (see Section 5).

The atmospheric CO_2 concentrations and the mean surface air temperatures are projected to increase, with a strong widening of the projection uncertainties (Figure 4). The temperature projections are relative to 1850, and are in the range of the recent IPCC results (Meehl et al., 2007). The AMOC intensity is projected to decrease considerably, with a sizeable probability of an AMOC collapse (defined here as an AMOC intensity of zero) in the considered time horizon. The mode of the AMOC reconstruction and projection decreases by approximately 35–40 percent from 1900 to 2100. This reduction is consistent with the

For Peer Review

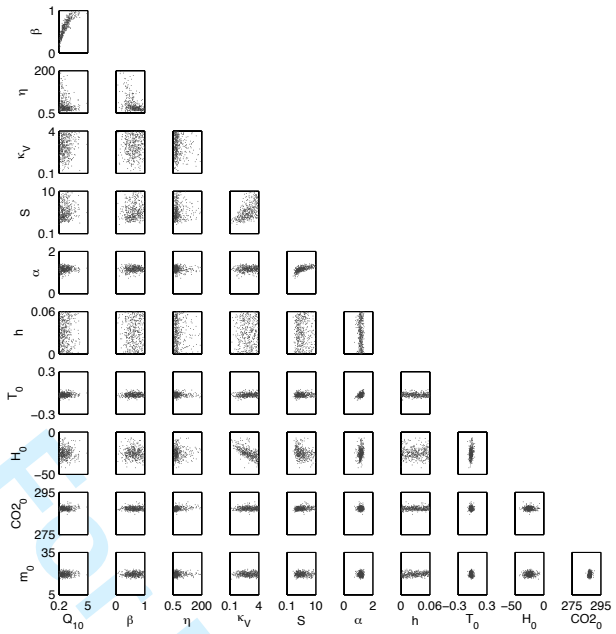

Figure 3. Two dimensional projections of the posterior probability density functions of the estimated model parameters derived from the data-model fusion illustrating the correlation in the posterior estimates.

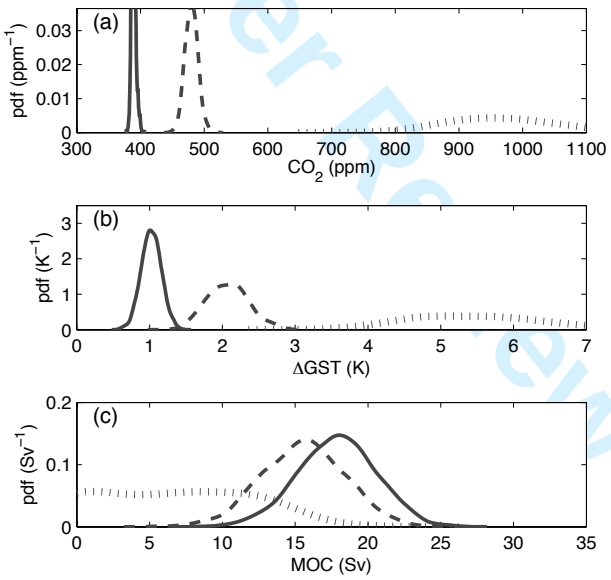

Figure 4. Probabilistic projections of (a) global mean surface temperature anomalies, (b) atmospheric CO_2 concentrations, and (c) AMOC strength in 2010 (solid), 2050 (dashed), and 2150 (dotted).

results of Schneider et al. (2007), and somewhat smaller than the results of Knutti et al. (2003), which show AMOC reductions of approximately 30 and 60 percent, respectively over the same time horizon. (The 2150 projections for AMOC strength include some negative values, not shown in the graph. This is due to the addition of observational noise, as the model itself does not produce AMOC reversals.)

An AMOC collapse has been interpreted as a low-probability event (Alley et al., 2007;

For Peer Review

Rahmstorf and Zickfeld, 2005; Wood et al., 2003). The model projections suggest that an AMOC collapse in the 21st century is very unlikely (i.e., a probability of less than ten percent, Figure 5, dashed curve), consistent with the recent IPCC assessment (Alley et al., 2007). (The AMOC is defined to be collapsed if the modeled AMOC strength, without added observation error, is zero.) However, the projected probability of an AMOC collapse increases sharply after 2100 to exceed 50 percent in the next two centuries in this very simple model.

Although the probability of experiencing an AMOC collapse in the 21st century is small according to our analysis, the probability of committing to a future collapse within the next century can be much higher. To test this, we explore several alternate forcing scenarios in which CO_2 emissions are abruptly reduced to zero in a given year and remain zero thereafter. An AMOC collapse is triggered by that year if the AMOC later collapses by 2300. Our analysis indicates that even if emissions are reduced to zero after 2050, there is nearly a ten percent chance that the AMOC will collapse by 2300 (Figure 5, solid curve). If CO_2 emissions stop in 2100, the probability of committing to an AMOC collapse rises to 40 percent.

It is important to stress that these projections are based on a single business-as-usual scenario for CO_2 emissions, and are hence silent on the effects of potential cuts in CO_2 emissions due to climate policies, as well as on the uncertainty in the future BAU emissions trajectory.

6 Caveats

The results of this proof-of-concept study hinge on a large number of simplifying assumptions that impose severe caveats on the forthcoming conclusions and point to potential future improvements. Relevant examples for such potential improvements include: (i) using a more refined Earth system model, (ii) considering information contained in the spatial structure of the observational constraints, (iii) representing the uncertainty in the CO_2 emissions scenarios, and (iv) adding paleo-proxies to the analyzed data set. These future research areas are briefly discussed below.

First, the adopted model is extremely simple and misses likely important feedbacks such as changes in the nitrogen cycle (Houghton et al., 1998) or the Greenland ice sheet dynamics (Zwally et al., 2002). Increasing the model complexity is a logical step to reduce this problem (e.g., Challenor et al., 2006), but many of these potentially relevant feedbacks are

For Peer Review

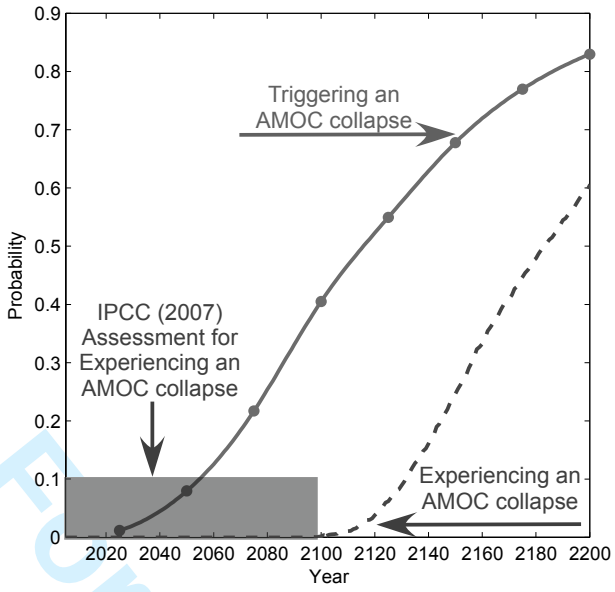

Figure 5. Model-derived risk estimate of a AMOC collapse over time. The dashed curve is the probability that the AMOC will be in a state of collapse in a given year. The solid curve depicts the commitment to future AMOC collapse, i.e., the probability of crossing a collapse threshold. It is the probability that if BAU emissions are reduced to zero beyond a given year, the AMOC will nevertheless be in a state of collapse in the year 2300. The shaded box represents the judgement of the 2007 IPCC Fourth Assessment Report (Alley et al., 2007), $< 10\%$ probability of collapse by 2100.

still poorly resolved in Earth system models. Second, our analysis considers only globally aggregate information (e.g., the global average surface air temperature). This approach reduces the computational burden considerably, but it neglects potentially useful information contained in the spatial signal structure. For example, the pattern of oceanic heat and other tracer anomalies may provide useful constraints on the ocean diffusivity (Cessi et al., 2006; Schmittner et al., 2008). Third, this study considers a single CO_2 emissions scenario to isolate the effects of key uncertainties in the carbon, climate, and AMOC system from the uncertainties in the socioeconomic system. The projections are hence contingent on the adopted CO_2 emissions scenario. Using probabilistic CO_2 emissions scenarios (Keller, Miltich, Robinson and Tol, 2007; Webster et al., 2002) would likely change the estimated probabilities of a future AMOC collapse. Last, but not least, this study uses century-scale observations that are mostly derived from the instrumental record. Adding paleo-observations such as reconstructed temperatures over a millennium time-scale may provide important additional constraints (Crowley, 2000; Hegerl et al., 2006).

7 Conclusions

We develop a simple and computationally efficient model of the coupled climate, carbon, and AMOC systems. We demonstrate the feasibility to calibrate this model using a Bayesian

For Peer Review

Table 1. Estimated model and data distributional parameters, and their prior ranges.

parameter	symbol	units	min.	max.
respiration sensitivity	Q_{10}	—	0.2	5
carbon fertilization factor	β	—	0	1
thermocline transfer rate	η	m yr^{-1}	0.5	200
vertical diffusivity	κ_V	cm^2 s^{-1}	0.1	4
climate sensitivity	S	K	0.1	10
aerosol scaling	α	—	0	2
hydrological sensitivity	h	Sv K^{-1}	0	0.06
init. temperature	T_0	K	-0.3	0.3
init. ocean heat	H_0	10^{22} J	-50	0
init. CO_2	CO_{2_0}	ppm	275	295
init. AMOC strength	m_0	Sv	5	35
autocorr. (T)	ρ_T	—	0	0.99
autocorr. (CO_2, inst.)	$\rho_{CO_2,\text{inst}}$	—	0	0.99
autocorr. (ocean heat)	ρ_H	—	0	0.99
std. dev. (T)	σ_T	K	0.05	0.5
std. dev. (CO_2, ice)	$\sigma_{CO_2,\text{ice}}$	ppm	0.2	20
std. dev. (CO_2, inst.)	$\sigma_{CO_2,\text{inst}}$	ppm	0.2	7
std. dev. (ocean heat)	σ_H	10^{22} J	0.1	10

inversion technique to derive probabilistic hindcasts and projections that carefully sample the tail areas of the parameter probability density function. The probability of an AMOC collapse in the 21st century under a business-as-usual CO_2 emissions scenario is less than ten percent in our simple model. This estimate is consistent with the recent IPCC assessment (Alley et al., 2007). However, the projected probability of an AMOC collapse increases considerably beyond the 21st century and exceeds 50 percent over the next three centuries. Although the probability of experiencing an AMOC collapse in the 21st century is low, the probability of crossing a forcing threshold and committing to a future collapse during this century is as high as 40 percent.

For Peer Review

8 Acknowledgements

We thank Kirsten Zickfeld and Elmar Kriegler for providing the source codes of the DOECLIM and the AMOC box models and for many insightful discussions. Funding for this project was provided by the U.S. Environmental Protection Agency under Purchase Order EP07H000339 and by the National Science Foundation (HSD 072 9413). Any opinions, findings and conclusions or recommendations expressed in this material, and remaining errors, are those of the authors and do not necessarily reflect the views of the funding entity.

REFERENCES

Adger, N., Aggarwal, P., Agrawala, S., Alcamo, J., Allali, A., Anisimov, O., Arnell, N., Boko, M., Canziani, O., Carter, T., Casassa, G., Confalonieri, U., Cruz, R. V., Alcaraz, E. d. A., Easterling, W., Field, C., Fischlin, A., Fitzharris, B. B., Garca, C. G., Hanson, C., Harasawa, H., Hennessy, K., Huq, S., Jones, R., Bogataj, L. K., Karoly, D., Klein, R., Kundzewicz,

Z., Lal, M., Lasco, R., Love, G., Lu, X., Magrn, G., J.Mata, L., McLean, R., Menne, B., Midgley, G., Mimura, N., Mirza, M. Q., Moreno, J., Mortsch, L., Niang-Diop, I., Nicholls, R., Novky, B., Nurse, L., Nyong, A., Oppenheimer, M., Palutikof, J., Parry, M., Patwardhan, A., Lankao, P. R., Rosenzweig, C., Schneider, S., Semenov, S., Smith, J., Stone, J., Ypersele, J.-P. v., Vaughan, D., Vogel, C., Wilbanks, T., Wong, P. P., Wu, S. and Yohe, G. 2007. Climate change 2007: Impacts, adaptation and vulnerability, summary for policymakers Adger, N., Aggarwal, P., Agrawala, S., Alcamo, J., Allali, A., Anisimov, O., Arnell, N., Boko, M., Canziani, O., Carter, T., Casassa, G., Confalonieri, U., Cruz, R. V., Alcaraz, E. d. A., Easterling, W., Field, C., Fischlin, A., Fitzharris, B. B., Garca, C. G., Hanson, C., Harasawa, H., Hennessy, K., Huq, S., Jones, R., Bogataj, L. K., Karoly, D., Klein, R., Kundzewicz, Z., Lal, M., Lasco, R., Love, G., Lu, X., Magrn, G., J.Mata, L., McLean, R., Menne, B., Midgley, G., Mimura, N., Mirza, M. Q., Moreno, J., Mortsch, L., Niang-Diop, I., Nicholls, R., Novky, B., Nurse, L., Nyong, A., Oppenheimer, M., Palutikof, J., Parry, M., Patwardhan, A., Lankao, P. R., Rosenzweig, C., Schneider, S., Semenov, S., Smith, J., Stone, J., Ypersele, J.-P. v., Vaughan, D., Vogel, C., Wilbanks, T., Wong, P. P., Wu, S. and Yohe, G. IPCC Secretariat, c/o WMO, 7bis, Avenue de la Paix, C.P. N ° 2300, 1211 Geneva 2, SWITZERLAND.

Alley, R., Berntsen, T., Bindoff, N. L., Chen, Z., Chidthaisong, A., Friedlingstein, P., Gregory, J., Hegerl, G., Heimann, M., Hewitson, B., Hoskins, B., Joos, F., Jouzel, J., Kattsov, V., Lohmann, U., Manning, M., Matsuno, T., Molina, M., Nicholls, N., Overpeck, J., Qin, D., Raga, G., Ramaswamy, V., Ren, J., Rusticucci, M., Solomon, S., Somerville, R., Stocker, T. F., Stott, P., Stouffer, R. J., Whetton, P., Wood, R. A. and Wratt, D. 2007. Climate change 2007: The physical science basis, summary for policymakers Alley, R., Berntsen, T., Bindoff, N. L., Chen, Z., Chidthaisong, A., Friedlingstein, P., Gregory, J., Hegerl, G., Heimann, M., Hewitson, B., Hoskins, B., Joos, F., Jouzel, J., Kattsov, V., Lohmann, U., Manning, M., Matsuno, T., Molina, M., Nicholls, N., Overpeck, J., Qin, D., Raga, G., Ramaswamy, V., Ren, J., Rusticucci, M., Solomon, S., Somerville, R., Stocker, T. F., Stott, P., Stouffer, R. J., Whetton, P., Wood, R. A. and Wratt, D. IPCC Secretariat, c/o WMO, 7bis, Avenue de la Paix, C.P. N ° 2300, 1211 Geneva 2, SWITZERLAND.

Baumgartner, A. and Reichel, E. 1975. The world water balance Baumgartner, A. and Reichel, E. Elsevier, Amsterdam, the Netherlands, and New York, USA.

Broecker, W. S. 1991. The great ocean conveyor. *Oceanography* **4**, 79–89.

Brohan, P., Kennedy, J. J., Harris, I., Tett, S. F. B. and Jones, P. D. 2006. Uncertainty estimates in regional and global observed temperature changes: A new data set from 1850. *Journal of Geophysical Research-Atmospheres* **111**(D12), –.

Bryden, H. L., Longworth, H. R. and Cunningham, S. A. 2005. Slowing of the Atlantic meridional overturning circulation at 25° N. *Nature Nature* **438**(7068), 655–657.

Cessi, P., Young, W. R. and Polton, J. A. 2006. Control of large-scale heat transport by small-scale mixing. *Journal of Physical Oceanography* **36**(10), 1877–1894.

Challenor, P. G., Hankin, R. K. S. and March, R.: 2006, *Avoiding dangerous climate change*, Cambridge University Press, pp. –.

Crowley, T. J. 2000. Causes of climate change over the past 1000 years. *Science* **289**(5477), 270–277.

Cunningham, S. A., Kanzow, T., Rayner, D., Baringer, M. O., Johns, W. E., Marotzke, J., Longworth, H. R., Grant, E. M., Hirschi, J. J. M., Beal, L. M., Meinen, C. S. and Bryden, H. L. 2007. Temporal variability of the Atlantic meridional overturning circulation at 26.5°N. *Science* **317**(5840), 935–938.

Curry, R. and Mauritzen, C. 2005. Dilution of the northern North Atlantic Ocean in recent decades. *Science* **308**(5729), 1772–1774.

Draper, D. 1995. Assessment and propagation of model uncertainty. *Journal of the Royal Statistical Society Series B-Methodological* **57**(1), 45–97.

Etheridge, D. M., Steele, L. P., Langenfelds, R. L., Francey, R. J., Barnola, J. M. and Morgan, V. I. 1996. Natural and anthropogenic changes in atmospheric CO_2 over the last 1000 years from air in Antarctic ice and firn. *Journal of Geophysical Research-Atmospheres* **101**(D2), 4115–4128.

Forest, C. E., Stone, P. H., Sokolov, A. P., Allen, M. R. and Webster, M. D. 2002. Quantifying uncertainties in climate system properties with the use of recent climate observations. *Science* **295**, 113–117.

For Peer Review

Friedlingstein, P., Cox, P., Betts, R., Bopp, L., von Bloh, W., Brovkin, V., Cadule, P., Doney, S., Eby, M., Fung, I., Bala, G., John, J., Jones, C., Joos, F., Kato, T., Kawamiya, M., Knorr, W., Lindsay, K., Matthews, H. D., Raddatz, T., Rayner, P., Reick, C., Roeckner, E., Schnitzler, K.-G., Schnur, R., Strassmann, K., Weaver, A. J., Yoshikawa, C. and Zeng, N. 2006. Climate-carbon cycle feedback analysis: Results from the C^4MIP model intercomparison. *Journal of Climate* **19**, 3337–3353.

Gouretski, V. and Koltermann, K. P. 2007. How much is the ocean really warming?. *Geophysical Research Letters* **34**, L01610.

Hastings, W. K. 1970. Monte Carlo sampling methods using Markov chains and their applications. *Biometrika* **57**(1), 97–109.

Hegerl, G. C., Crowley, T. J., Hyde, W. T. and Frame, D. J. 2006. Climate sensitivity constrained by temperature reconstructions over the past seven centuries. *Nature* **440**(7087), 1029–1032.

Hoeting, J. A., Madigan, D., Raftery, A. E. and Volinsky, C. T. 1999. Bayesian model averaging: A tutorial. *Stat Sci* **14**(4), 382–401.

Hooss, G., Voss, R., Hasselmann, K., Maier-Reimer, E. and Joos, F. 2001. A nonlinear impulse response model of the coupled carbon cycle-climate system (NICCS). *Climate Dynamics* **18**(3-4), 189–202.

Houghton, R. A., Davidson, E. A. and Woodwell, G. M. 1998. Missing sinks, feedbacks, and understanding the role of terrestrial ecosystems in the global carbon balance. *Global Biogeochemical Cycles* **12**(1), 25–34.

Jain, A. K. and Yang, X. J. 2005. Modeling the effects of two different land cover change data sets on the carbon stocks of plants and soils in concert with CO_2 and climate change. *Global Biogeochemical Cycles* **19**(2), –.

Kanzow, T., Cunningham, S. A., Rayner, D., Hirschi, J. J. M., Johns, W. E., Baringer, M. O., Bryden, H. L., Beal, L. M., Meinen, C. S. and Marotzke, J. 2007. Observed flow compensation associated with the MOC at 26.5°N in the Atlantic. *Science* **317**(5840), 938–941.

Keeling, C. D. and Whorf, T. P. 2005. Atmospheric CO_2 records from sites in the SIO air sampling network, *Technical report*, Carbon Dioxide Information Analysis Center, Oak Ridge National Laboratory.

Keller, K., Bolker, B. M. and Bradford, D. F. 2004. Uncertain climate thresholds and optimal economic growth. *Journal of Environmental Economics and Management* **48**, 723–741.

Keller, K. and McInerney, D. 2008. The dynamics of learning about a climate threshold. *Climate Dynamics* **30**, 321–332.

Keller, K., Miltich, L. I., Robinson, A. and Tol, R. S. J. 2007. How overconfident are current projections of carbon dioxide emissions?. *Working Paper Series, Research Unit Sustainability and Global Change, Hamburg University.* **FNU-124**, http://ideas.repec.org/s/sgc/wpaper.html.

Keller, K., Schlesinger, M. and Yohe, G. 2007. Managing the risks of climate thresholds: Uncertainties and information needs. *Climatic Change* pp. Published online: 23 January 2007, http://dx.doi.org/10.1007/s10584–006–9114–6.

Keller, K., Tan, K., Morel, F. M. M. and Bradford, D. F. 2000. Preserving the ocean circulation: Implications for climate policy. *Climatic Change* **47**(1-2), 17–43.

Knutti, R. and Stocker, T. F. 2002. Limited predictability of the future thermohaline circulation close to an instability threshold. *Journal of Climate* **15**, 179–186. 10.1175/1520-0442(2002)015$⟨$0179:LPOTFT$⟩$2.0.CO;2.

Knutti, R., Stocker, T. F., Joos, F. and Plattner, G. K. 2003. Probabilistic climate change projections using neural networks. *Climate Dynamics* **21**(3-4), 257–272.

Kriegler, E.: 2005, PhD thesis, Potsdam.

Latif, M., Roeckner, E., Mikolajewski, U. and Voss, R. 2000. Tropical stabilization of the thermohaline circulation in a greenhouse warming simulation. *Journal of Climate* **13**, 1809–1813.

Link, P. M. and Tol, R. S. J. 2004. Possible economic impacts of a shutdown of the thermohaline circulation: an application of FUND. *Portuguese Economic Journal* **3**, 99–114.

Lumpkin, R. and Speer, K. 2007. Global ocean meridional overturning. *Journal of Physical Oceanography* **37**(10), 2550–2562.

Manabe, S. and Stouffer, R. J. 1994. Multiple-century response of a coupled ocean-atmosphere model to an increase of atmospheric carbon dioxide. *Journal of Climate* **7**, 5–23. 10.1175/1520-0442(1994)007$⟨$0005:MCROAC$⟩$2.0.CO;2.

Marland, G., Boden, T. and Andres, R.: 2004, *Trends: A Compendium of Data on Global Change*, Carbon Dioxide Information Analysis Center, Oak Ridge National Laboratory, U.S. Department of Energy, Oak Ridge, TN, U.S.A. Available electronically

For Peer Review

from: http://cdiac.ornl.gov/trends.

McNeil, B. I., Matear, R. J., Key, R. M., Bullister, J. L. and Sarmiento, J. L. 2003. Anthropogenic CO_2 uptake by the ocean based on the global chlorofluorocarbon data set. *Science* **299**(5604), 235–239.

Meehl, G. A., Stocker, T. F., Collins, W. D., Friedlingstein, P., Gaye, A., Gregory, J., Kitoh, A., Knutti, R., Murphy, J., Noda, A., Raper, S., Watterson, I., Weaver, A. and Zhao, Z.-C.: 2007, *Climate Change 2007: The Physical Science Basis. Contribution of Working Group I to the Fourth Assessment Report of the Intergovernmental Panel on Climate Change*, Cambridge University Press, Cambridge, United Kingdom and New York, NY, USA., pp. –.

Metropolis, N., Rosenbluth, A. W., Rosenbluth, M. N., Teller, A. H. and Teller, E. 1953. Equation of state calculations by fast computing machines. *J. Chem. Phys.* **21**, 1087–1092.

Nordhaus, W. D. 2007. The challenge of global warming: Economic models and environmental policy, *Technical report*, `http://nordhuas.econ.yale.edu/DICE2007.htm`, accessed May 2, 2007, model version: DICE-2007.delta.v7.

Rahmstorf, S. and Zickfeld, K. 2005. Thermohaline circulation changes: A question of risk assessment - an editorial review essay. *Climatic Change* **68**(1-2), 241–247.

Ramankutty, N. and Foley, J. A. 1999. Estimating historical changes in global land cover: Croplands from 1700 to 1992. *Global Biogeochemical Cycles* **13**(4), 997–1027.

Ricciuto, D., Davis, K. and Keller., K. 2008. A Bayesian calibration of a simple carbon cycle model: The role of observations in estimating and reducing uncertainty. *Global Biogeochemical Cycles* **22**, GB2030.

Schmittner, A., Urban, N. M., Keller, K. and Matthews, D. 2008. Using tracer observations to reduce the uncertainty of ocean diapycnal mixing and climate-carbon cycle projections. *Global Biogeochemical Cycles* . (in review, e-print available at `http://www.geosc.psu.edu/~kkeller/Schmittner_et_al_gbc_08.pdf`).

Schneider, B., Latif, M. and Schmittner, A. 2007. Evaluation of different methods to assess model projections of the future evolution of the Atlantic meridional overturning circulation. *Journal of Climate* **20**(10), 2121–2132.

Stocker, T. F., Clarke, G., Treut, H. L., Lindzen, R., Meleshko, V., Mugara, R., Palmer, T., Pierrehumbert, R., Sellers, P., Trenberth, K., Willebrand, J., Alley, R., Anisimov, O., Appenzeller, C., Barry, R., Bates, J., Bindschadler, R., Bonan, G., Bning, C., Bony, S., Bryden, H., Cane, M., Curry, J., Delworth, T., Denning, A., Dickinson, R., Echelmeyer, K., Emanuel, K., Flato, G., Fung, I., Geller, M., Gent, P., Griffies, S., Held, I., Henderson-Sellers, A., Holtslag, A., Hourdin, F., Hurrell, J., Kattsov, V., Killworth, P., Kushnir, Y., Large, W., Latif, M., Lemke, P., Mann, M., Meehl, G., Mikolajewicz, U., OHirok, W., Parkinson, C., Payne, A., Pitman, A., Polcher, J., Polyakov, I., Ramaswamy, V., Rasch, P., Salathe, E., Schr, C., Schmitt, R., Shepherd, T., Soden, B., Spencer, R., Taylor, P., Timmermann, A., Vinnikov, K., Visbeck, M., Wijffels, S., Wild, M., Manabe, S. and Mason, P.: 2001, *Climate Change 2001: The Scientific Basis, Contribution of Working Group I to the Third Assessment Report of the Intergovernmental Panel on Climate Change*, Cambridge University Press, Cambridge, UK, pp. 417–470.

Stommel, H. 1961. Thermohaline convection with two stable regimes of flow. *Tellus* **13**(2), 224–230.

Stouffer, R. J., Yin, J., Gregory, J. M., Dixon, K. W., Spelman, M. J., Hurlin, W., Weaver, A. J., Ebyd, M., Flato, G. M., Hasumi, H., Hu, A., Jungclaus, J. H., Kamenkovich, I. V., Levermann, A., Montoya, M., Murakami, S., Nawrath, S., Oka, A., Peltier, W. R., Robitaille, D. Y., Sokolov, A., Vettoretti, G. and Weber, S. L. 2006. Investigating the causes of the response of the thermohaline circulation to past and future climate changes. *Journal of Climate* **19**(8), 1365–1387.

Tanaka, K. and Kriegler, E. 2007. Aggregated carbon cycle, atmospheric chemistry, and climate model (ACC2). description of the forward and inverse modes, *Technical report*, Hamburg (Germany).

Urban, N. M. and Keller, K. 2008. Complementary constraints on climate sensitivity. *Geophysical Research Letters* . (in review, e-print available at `http://www.geosc.psu.edu/~kkeller/Urban_Keller_grl_08_submitted.pdf`).

Vellinga, M. and Wood, R. A. 2002. Global climatic impacts of a collapse of the Atlantic thermohaline circulation. *Climatic Change* **54**(3), 251–267.

Webster, M. D., Babiker, M., Mayer, M., Reilly, J. M., Harnisch, J., Hyman, R., Sarofim, M. C. and Wang, C. 2002. Uncertainty in emissions projections for climate models. *Atmos. Environ.* **36**(22), 3659–3670.

For Peer Review

Wood, R. A., Vellinga, M. and Thorpe, R. 2003. Global warming and thermohaline circulation stability. *Philosophical Transactions of the Royal Society of London Series a-Mathematical Physical and Engineering Sciences* **361**(1810), 1961–1974.

Yohe, G., Schlesinger, M. E. and Andronova, N. G. 2006. Reducing the risk of a collapse of the Atlantic thermohaline circulation. *The Integrated Assessment Journal* **6**(1), 57–73.

Zellner, A. and Tiao, G. C. 1964. Bayesian analysis of the regression model with autocorrelated errors. *Journal of the American Statistical Association* pp. 763–778.

Zickfeld, K., Slawig, T. and Rahmstorf, S. 2004. A low-order model for the response of the atlantic thermohaline circulation to climate change. *Ocean Dynamics* **54**(1), 8–26.

Zwally, H. J., Abdalati, W., Herring, T., Larson, K., Saba, J. and Steffen, K. 2002. Surface melt-induced acceleration of greenland ice-sheet flow. *Science* **297**(5579), 218–222.

For Peer Review